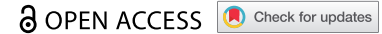


RESEARCH PAPER



## Mechanism of microRNA regulating the progress of atherosclerosis in apoE-deficient mice

Xiaoqian Lou<sup>a,b</sup>, Dawei Wang<sup>c</sup>, Zehui Gu<sup>d</sup>, Tengteng Li<sup>a</sup>, and Liqun Ren<sup>a</sup>

<sup>a</sup>Department of Experimental Pharmacology and Toxicology, School of Pharmacy, Jilin University, Changchun, Jilin, China; <sup>b</sup>Department of Endocrinology, The First Hospital of Jilin University, Changchun, Jilin, People's Republic of China; <sup>c</sup>Department of Emergency, The First Hospital of Jilin University, Changchun, Jilin, People's Republic of China; <sup>d</sup>Department of Pathology, The Third Affiliated Hospital of Jinzhou Medical University, Jinzhou, People's Republic of China

### ABSTRACT

MicroRNAs play important roles in atherosclerogenesis and are important novel pharmaceutical targets in atherosclerosis management. The whole spectrum of miRNAs dysregulation is still under intense investigation. This study intends to identify more novel dysregulated microRNAs in atherosclerotic mice. Half of eight-week-old male ApoE<sup>-/-</sup> mice were fed with high-fat-diet for 12 weeks as a model mice, and the remaining half of ApoE<sup>-/-</sup> mice were fed with a normal-diet as a control. A serum lipid profile was performed with ELISA kits, and atherosclerotic lesions were assessed. Aortic tissues were dissected for gene expression profiling using a Multispecies miRNA 4.0 Array, and significant differentially expressed miRNAs were identified with fold change  $\geq 2$  and  $p < 0.05$ . Real-time quantitative PCR was used to validate microarray gene expression data on selected genes. Predicted target genes were extracted and subjected to bioinformatic analysis for molecular function and pathway enrichment analysis. Model mice showed a 15.32% atherosclerotic lesion compared to 1.52% in the control group. A total of 25 significant differentially expressed microRNAs were identified, with most of them (24/25) downregulated. Real-time quantitative PCR confirmed the GeneChip data. Bioinformatic analysis of predicted target genes identified high involvement of the PI3K/Akt/mTOR signaling pathway. Microarray profiling of miRNAs in high-fat-fed Model mice identified 25 differentially expressed miRNAs, including some novel miRNAs, and the PI3K/Akt/mTOR signaling pathway is highly enriched in the predicted target genes. The novel identified dysregulated miRNAs suggest a broader spectrum of miRNA dysregulation in the progression of atherosclerosis and provide more research and therapeutic targets for atherosclerosis.

### ARTICLE HISTORY

Received 8 October 2021  
Revised 5 November 2021  
Accepted 5 November 2021

### KEYWORDS



MicroRNA; Atherosclerosis; ApoE-deficient mouse; Gene regulation; Bioinformatic analysis

## Introduction

Atherosclerosis is well known as the leading cause of human mortality [1,2]. The development of atherosclerosis is a chronic inflammatory process involving pathological changes in vascular endothelial cells [3,4], monocytes/macrophages [5,6], and vascular smooth muscle cells [7,8]. Beyond those identified risk factors, including hypertension, hyperlipidemia, diabetes, inflammation, and oxidative stress [9–13], the fundamental mechanisms are still under extensive investigation.

MicroRNAs (miRs) are short non-coding RNAs (~22nt in length), which regulate gene expression by degrading target mRNAs and/or inhibiting their translation and have important roles in atherosclerogenesis [14–18]. Wide ranges of dysregulated miRNAs identified from different sources, like

serum, atherosclerotic tissue, endothelium cells, vascular smooth muscle cells, and subsets of macrophages, exert broad pathological effects on atherosclerogenesis through effects on endothelial cells [19–22], inflammatory cells/macrophages [23–26], vascular smooth muscle cells [27–31], and lipid metabolism [32–34]. MicroRNAs are new biomarkers and potential therapeutic targets in atherosclerosis. ApoE knockout (ApoE<sup>-/-</sup>) mice have been widely used as an atherosclerotic animal model to identify and test dysregulated miRNAs during atherosclerogenesis. Different sets of dysregulated miRNAs were identified by researchers using ApoE<sup>-/-</sup> mice fed with a Western-type diet (21% fat). Like Han [35] identified 75 differentially expressed miRNAs from pooled atherosclerotic aortic tissues of 8-month-old ApoE<sup>-/-</sup> mice, and Zhen [36] identified 9 (at

**CONTACT** Liqun Ren  [renlq@jlu.edu.cn](mailto:renlq@jlu.edu.cn)  Department of Experimental Pharmacology and Toxicology, School of Pharmacy, Jilin University, Xinmin Avenue1163, Changchun, Jilin Province 130021, China

© 2021 The Author(s). Published by Informa UK Limited, trading as Taylor & Francis Group.  
This is an Open Access article distributed under the terms of the Creative Commons Attribution License (<http://creativecommons.org/licenses/by/4.0/>), which permits unrestricted use, distribution, and reproduction in any medium, provided the original work is properly cited.

8 weeks) and 19 (at 20 weeks) differentially expressed miRNAs at different stages from atherosclerotic aortic tissues. ApoE<sup>-/-</sup> mice fed with a high-fat diet (40% fat) show early and extensive atherosclerosis lesions, and various dysregulated miRNAs are reported, such as miRNA-155 [37], miRNA-26a-5p [38], miR-6931-5p, mmu-miR-3547-5p, mmu-miR-5107-5p, mmu-miR-6368, and mmu-miR-7118-5p in aorta atherosclerotic lesions [39]. The continuous identification of novel dysregulated miRNAs suggests dynamic regulation of miRNAs in the progress of atherosclerogenesis, but the whole spectrum of miRNA regulation during the process of atherosclerosis is still unclear. This study intends to identify more novel dysregulated microRNAs in atherosclerotic ApoE<sup>-/-</sup> mice. The aim is to provide more research and therapeutic targets for atherosclerosis. We report here additional novel dysregulated miRNAs in ApoE<sup>-/-</sup> mice fed with a high-fat diet for 12 weeks and bioinformatic analysis on predicted target genes.

## Materials and methods

### Animal model establishment

Eight-week-old male ApoE homozygous deficient (ApoE<sup>-/-</sup>) mice were obtained from HuaFuKang Bioscience (Beijing, China). Half of the ApoE<sup>-/-</sup> mice were used as a control and fed with a regular chow diet, and the remaining half of ApoE<sup>-/-</sup> mice were fed with a high-fat diet containing 40% kcal fat (cocoa butter and soybean oil) and 1.25% kcal cholesterol (HFD, D12108C, Research Diets Inc.) for 12 weeks. This study was approved by Jilin University Laboratory Animal Ethics Committee (Changchun, China), and all animal-related procedures were performed in accordance with Chinese regulations on the use of laboratory animals.

### Serum lipid profile

Blood samples were collected from the eyeballs after administering anesthesia, and the serum was isolated by centrifugation at 2500 rpm for 15 minutes. Total cholesterol (TC), triglyceride (TG), high density lipoprotein cholesterol (HDL-C), low density lipoprotein cholesterol (LDL-C), and oxidized low density lipoprotein (ox-LDL) levels were determined using commercial ELISA kits

acquired from Nanjing Jiancheng Bioengineering Institute (Nanjing, China).

### Atherosclerotic lesion assessment

The entire aorta (from the aortic root to the iliac artery) was dissected after initial perfusion (cold 1× phosphate buffer saline) through the left ventricle. For atherosclerotic lesion assessment, the section between the aortic arch and the common iliac artery was fixed in 4% paraformaldehyde for 24 hours and subjected to Oil Red O-staining as described [40]. After staining, the aorta was longitudinally opened to visualize the atherosclerotic lesions stained in red. Digital photos were taken using a digital camera (Canon EOS80D, Tokyo, Japan) and subjected to image analysis using Image-pro Plus 6.0 software (NIH Image, USA). The area of the atherosclerotic lesions was calculated as a percentage of the Oil Red O positive area. Aorta specimens were also fixed with buffered formalin solution and subjected to H&E staining.

### MicroRNA microarray analysis

The whole aorta tissues (3 in each groups) dissected free of surrounding tissues were washed with diethyl pyrocarbonate-treated phosphate buffer saline and snapped frozen in liquid nitrogen. The total RNA was isolated with TRIzol reagent (Invitrogen, Carlsbad, Canada) combined with RNeasy Mini Kit (Qiagen, Hilden, Germany). MicroRNA profiling was performed using the Multispecies miRNA 4.0 Array (Affymetrix GeneChip®, USA) at the service of CNKINGBIO (Beijing, China). Briefly, 130 ng of total RNA was used for cRNA synthesis, and the cRNA was hybridized for 16 hours at 45°C following fragmentation. GeneChips were washed and stained using Affymetrix Fluidics Station 450 and then scanned using GeneChip® Scanner 3000 7 G.

### Differentially expressed microRNAs

The microarray data were first analyzed using microarray analyze software at the service of CNKINGBIO (Beijing, China) based on a median summarization normalization method and the random variance model t-test. The differentially expressed miRNAs were extracted with p-values lower than 0.05 and

a fold change of at least 2. Differentially expressed miRNAs were subjected to further analysis using Cluster 3.0 and Treeview v1.60.

### Real-Time Quantitative Polymerase Chain Reaction (RT-qPCR)

RT-qPCRs were performed on eight differentially expressed microRNAs to verify the GeneChip analysis data. Briefly, first-strand cDNA Synthesis was done using M-MLV Reverse Transcriptase (Promega, WI, USA), and RT-qPCRs were performed using SYBR Green kit (Takara, Dalian, China) on ABI 7500 real-time PCR system (Applied Biosystems, Foster City, CA, USA). The normalized relative gene expression level was calculated based on the  $2^{-\Delta\Delta Ct}$  method [41] using 18S RNA as an endogenous control. The primers used for RT-qPCR are listed in Table 1.

### Target gene prediction of differentially expressed miRNAs

Differentially expressed microRNAs with more than a 2-fold change were used to pull predicted target genes from TargetScanMouse 7.1 (TargetScan.org) [42] and the miRanda database (microRNA.org) [43]. The common predicted target genes pulled from both databases were used to construct a regulatory network. The relationship strength, which indicates the network characteristic value, was calculated based on the functional

microRNA position in the network. The microRNAs with the highest eigenvalues were placed at pivotal positions in the network, and these microRNAs bear the strongest regulatory ability.

### Gene ontology and pathway enrichment analyses

The predicted target genes were subjected to Gene Ontology (GO: <http://www.geneontology.org>) analysis to map the molecular and biological functional GO terms. A high enrichment score indicates that a GO term is more vulnerable to experimental factors. Kyoto Encyclopedia of Genes and Genomes (KEGG; <http://www.genome.jp/kegg/>) was explored to analyze the enrichments of functional pathways and networks. The interaction networks between significant pathways and differentially expressed miRNAs were constructed based on a two-sided Fisher's exact test [44] and a  $\chi^2$  test [45].

### Statistical analysis

SPSS 22.0 software (SPSS Inc., Chicago, IL, USA) was used for statistical analysis. All data, including Oil Red O stain, RT-qPCR, and lipid profiling were analyzed using a student's *t* test [46], and presented as the mean plus or minus the standard deviation.

**Table 1.** Primer sequences used for qRT-PCR.

Gene	primer (5'→3')
mmu-miR-322-5p	RT Primer: GTCGTATCCAGTGCAGGGTCCGAGGTATTCGCACTGGATACGACTCCTCAA Forward: GCGCAGCAGCAATTCATGT
mmu-miR-674-3p	RT Primer: GTCGTATCCAGTGCAGGGTCCGAGGTATTCGCACTGGATACGACTTGTT Forward: GCGCAGCTCCCATCTCA
mmu-miR-30 c-2-3p	RT Primer: GTCGTATCCAGTGCAGGGTCCGAGGTATTCGCACTGGATACGACAGAGTA Forward: CGCTGGGAGAAGGCTGTT
mmu-miR-30e-3p	RT Primer: GTCGTATCCAGTGCAGGGTCCGAGGTATTCGCACTGGATACGACGCTGTA Forward: GCGCTTTCAGTCGGATGTT
mmu-miR-208a-5p	RT Primer: GTCGTATCCAGTGCAGGGTCCGAGGTATTCGCACTGGATACGACGTATAA Forward: GAGCTTTTGGCCCCGGG
mmu-miR-672-5p	RT Primer: GTCGTATCCAGTGCAGGGTCCGAGGTATTCGCACTGGATACGACTCACAC Forward: CGCGTGAGGTTGGTGTACTGT
mmu-miR-7001-5p	RT Primer: GTCGTATCCAGTGCAGGGTCCGAGGTATTCGCACTGGATACGACATGCTC Forward: GAGGCAGGGTGTGAGCGT
mmu-miR-434-3p	RT Primer: GTCGTATCCAGTGCAGGGTCCGAGGTATTCGCACTGGATACGACAGGAGT Forward: CGCGTTTGAACCATCACTCG

## Results

The whole spectrum of miRNA regulation during the process of atherosclerosis is still unclear. This study intends to identify more novel dysregulated microRNAs in atherosclerotic mice. The aim is to provide more research and therapeutic targets for atherosclerosis. We report here additional novel dysregulated miRNAs in ApoE<sup>-/-</sup> mice fed with a high-fat diet for 12 weeks and bioinformatic analysis on predicted target genes.

### **High-fat diet apoE<sup>-/-</sup> mice developed more significant atherosclerotic lesions**

Compared to the control mice, ApoE<sup>-/-</sup> mice fed with a high-fat diet exhibited significant development of atherosclerotic plaques as demonstrated using Oil Red O stain. A wide distribution of atherosclerotic lesions was observed throughout the entire aorta tree in ApoE<sup>-/-</sup> mice fed with a high-fat diet, and limited lesions were observed in the aortic root area in control mice (Figure 1(A)). The area of aorta atherosclerotic lesions in ApoE<sup>-/-</sup> mice fed with a high-fat diet was significantly higher than that of the control mice (15.32% vs 1.52%,  $p < 0.01$ , Figure 1(B)). H&E staining showed extensive lesions in ApoE<sup>-/-</sup> mice fed with a high-fat diet (Figure 1(C-D)).

### **ApoE<sup>-/-</sup> mice fed with a high-fat diet exhibited hyperlipidemia with regular HDL-C**

Serum lipid profiling showed significant hyperlipidemia in ApoE<sup>-/-</sup> mice fed with a high-fat diet, with serum levels of TC, TG, LDL-C, and ox-LDL significantly increased compared to the control group, and there was no change in HDL-C (Table 2).

### **Differentially expressed miRs and predicted target genes**

Microarray data analysis with significant filters (fold change  $\geq 2$ ,  $p < 0.05$ ) identified 25 differentially expressed miRs in ApoE<sup>-/-</sup> mice fed with a high-fat diet (Table 3), among which 24 miRs were downregulated, only mmu-miR-7001-5p was found to be upregulated. The most downregulated miR was mmu-miR-375-3p (fold change = -13.9). Hierarchical clustering analysis showed distinct expression patterns

between two groups (Figure 2(A)). A scatter plot map and the Volcano plot map were also used to assess the differential expression patterns of microarray data (Figure 2(B-C)). A few cores differentially expressed microRNAs, and their respective target genes were shown (Figure 2(D)).

### **GO enrichment analysis**

Common predicted target genes extracted from TargetScan and miRanda databases were subjected to GO analysis. The up-regulated miR target genes were found to be highly involved in protein binding, protein heterodimerization activity, metal ion binding, protein domain-specific binding, nucleotide-binding, and ATP binding (Figure 3(B)). Downregulated miRNA target genes showed significant enriched molecular functions in protein binding, metal ion binding, DNA binding, nucleotide binding, transferase activity, and ATP binding (Figure 3(B)).

### **Pathway enrichment analysis**

A microRNA target gene pathway enrichment analysis helps to understand the metabolic pathways (Figure 4(A-D)). According to the statistical results, we found that the up-regulated miR target genes showed pathway enrichment in cancer, cholinergic synapse, circadian entrainment, small cell lung cancer, and amphetamine addiction (Figure 5(A)). Downregulated miR target genes showed pathway enrichments in axon guidance, long-term potentiation, glioma, non-small lung cancer, and mTOR signaling pathway (Figure 5(B)).

### **RT-qPCR validation**

Eight differentially expressed miRs were selected for further RT-qPCR validation. RT-qPCR confirmed significant downregulation of miR-322-5p, miR-674-3p, miR-30 c-2-3p, miR-208a-5p, miR-672-5p, miR-434-3p, and miR-30e-3p, and upregulation of miR-7001-5p (Figure 6).

## Discussion

An ApoE<sup>-/-</sup> knockout mice model has long been used as an atherosclerogenic model which develops atherosclerosis lesions in the middle-to-large

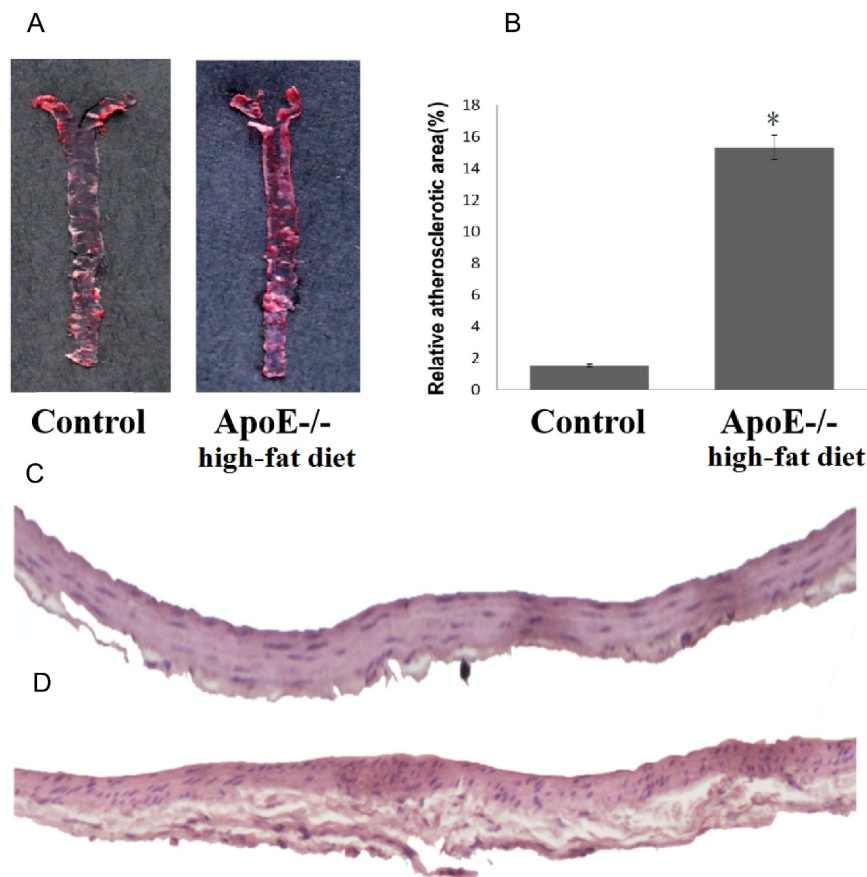


**Figure 1.** ApoE<sup>-/-</sup> mice fed with a high-fat diet exhibit a more pronounced atherosclerotic plaque. A: Oil Red O staining of atherosclerotic lesions in ApoE<sup>-/-</sup> mice fed with a high-fat diet and control mice. B: Quantitative lesion areas (Oil Red O positive) are calculated as a percentage of total aorta surface and presented as the mean  $\pm$  standard deviation of the mean (%), \* $p < 0.05$ ; There were three mice in each group. C: H&E stained transverse sections of the aortic arch in control (100 $\times$ ). D: H&E stained transverse sections of the aortic arch in ApoE<sup>-/-</sup> mice fed with a high-fat diet (100 $\times$ ).

**Table 2.** ApoE<sup>-/-</sup> mice fed with a high-fat diet exhibited higher levels of serum lipids except for HDL-C.

	TC (mmol/L)	TG (mmol/L)	HDL-C (mmol/L)	LDL-C (mmol/L)	Ox-LDL (mmol/L)
Control	2.66 $\pm$ 0.31	0.79 $\pm$ 0.18	2.81 $\pm$ 0.24	7.47 $\pm$ 1.99	16.8 $\pm$ 1.90
ApoE <sup>-/-</sup> high-fat diet	30.13 $\pm$ 4.25*	4.52 $\pm$ 0.76*	2.67 $\pm$ 0.19	14.67 $\pm$ 1.62*	30.67 $\pm$ 1.10*

\* $p < 0.05$ .

arterial tree. A Western-type diet or a high-fat diet significantly speeds up the atherosclerotic lesion and distribution [47,48]. In our study, after a 12-week high fat diet, ApoE<sup>-/-</sup> mice fed with a high-fat diet exhibited a hyperlipidemia profile with increased serum TC, TG, LDL-C, and ox-LDL, and extensive atherosclerotic lesions on the aorta tree compared to the control group, which showed limited lesions in the aortic root and arch region.

Atherosclerosis is a prolonged chronic inflammatory process; the complexity of

atherosclerosis involves endothelia dysfunction, inflammatory response, macrophage infiltration/polarization, vascular smooth muscle cells dedifferentiation, and lipid dysregulation. ApoE<sup>-/-</sup> mice fed with a high-fat diet are widely used for miRs profiling, regulatory, and therapeutic targeting studies related to atherosclerosis [35,49,36,39,50]. An increasing list of dysregulated miRs in the ApoE<sup>-/-</sup> mice with a high-fat diet model under different conditions reveals a dynamic, time, and stimuli dependent regulation spectra. With significant

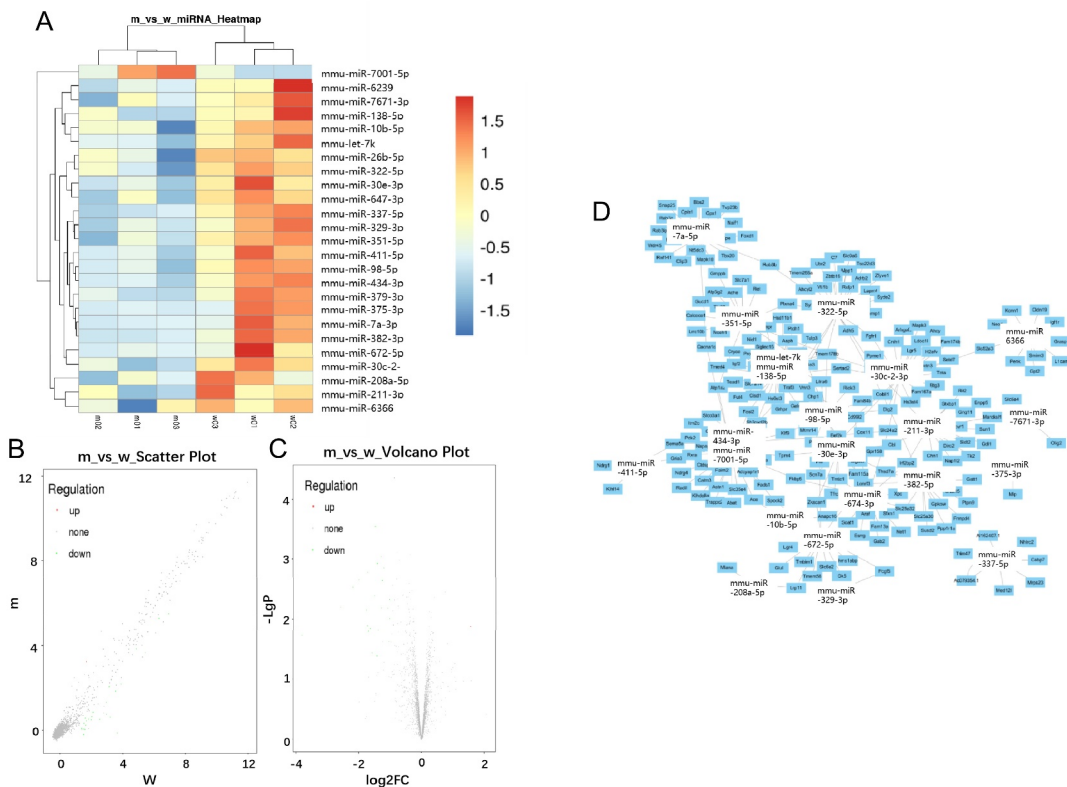


**Figure 2.** MiRNAs expression profiling using GeneChip analysis. A: Hierarchical cluster analysis of differentially expressed miRNAs ( $p < 0.05$ ;  $n = 3$ ). B: Scatter plot map of differentially expressed miRNAs. Upregulated miRNAs were marked in red, and downregulated miRNAs were marked in green ( $p < 0.05$ ;  $n = 3$ ). C: The volcano map overall gene expression. D: Predicted target genes of 24 differentially expressed miRNAs.

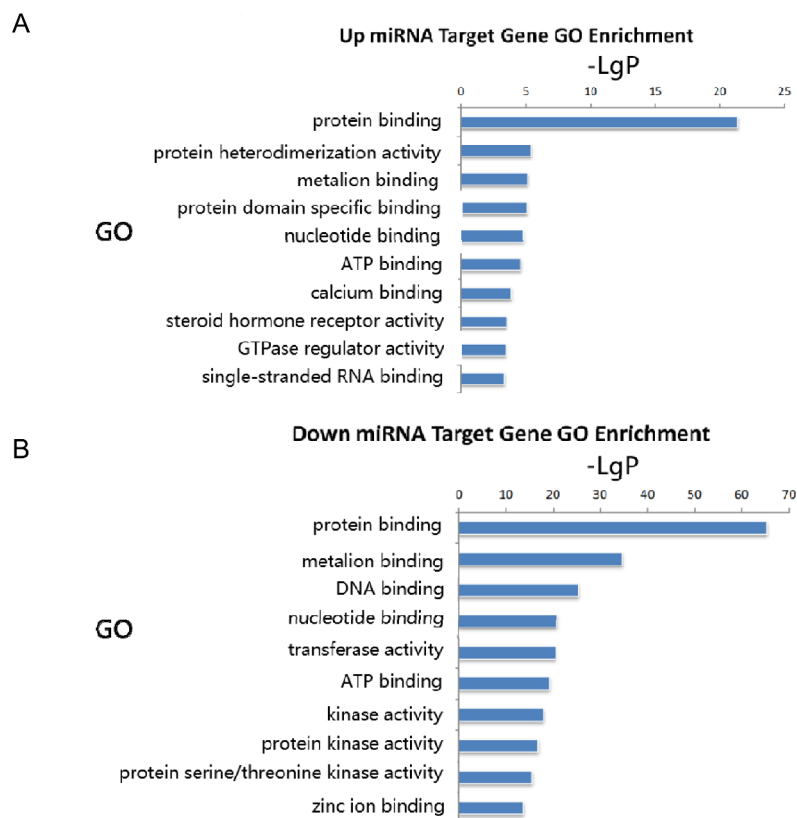


**Figure 3.** Gene ontology molecular function enrichment analyses of predicted target genes. A: Target genes of upregulated miRNA. B: Target genes of downregulated miRNAs.

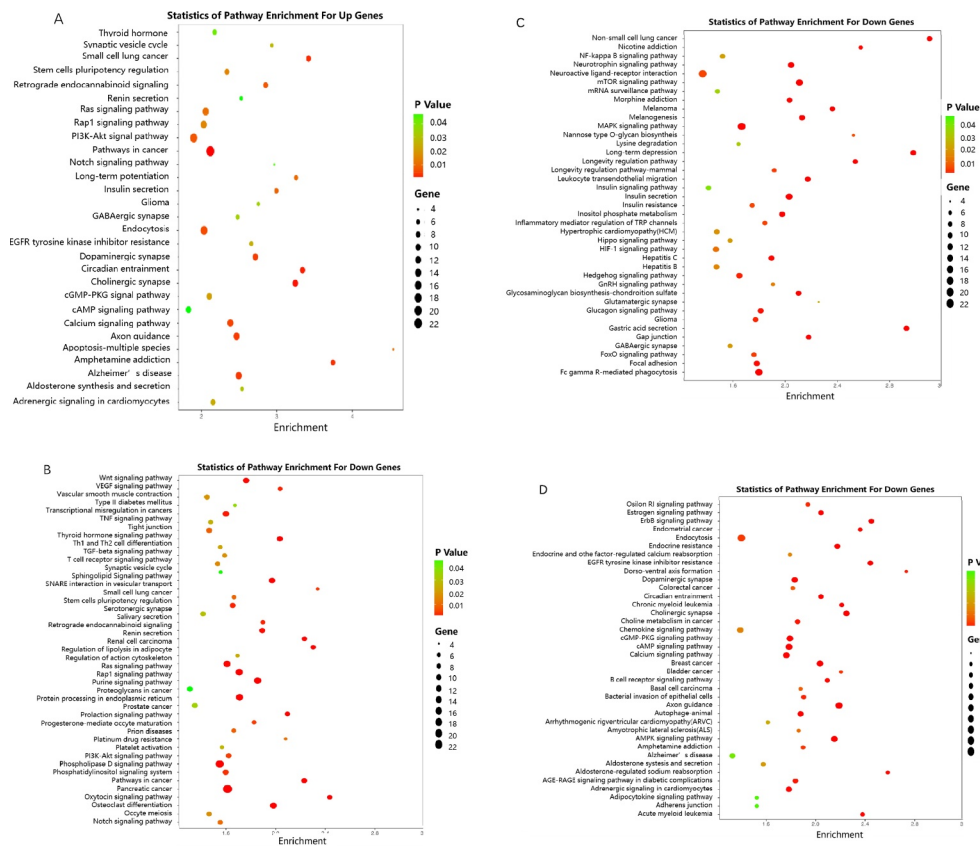


**Figure 4.** Pathway enrichment analyses of predicted target genes. A: Target genes of up regulated miRNAs. B-D: Target genes of down regulated miRNA.

atherosclerotic lesions at 12 weeks, we identified a total of 25 significantly differentially expressed microRNAs in ApoE<sup>-/-</sup> mice with a high-fat diet using GeneChip profiling, with most being down-regulated (24 of 25) and one being up-regulated. The most down-regulated miRNAs identification is very similar to a report on rats fed with a high-fat and high-sucrose diet for 4 weeks [51], which found 28 out of 29 down-regulated miRNAs. Among them, there are common miRNAs identified previously and newly identified miRNAs. Zhen identified a total of 28 dysregulated miRNAs at different stages of atherosclerosis in ApoE<sup>-/-</sup> mice fed with a Western-type diet [36]. miR-434-3p was down-regulated in both experiments. miR-434-3p plays a regulatory role in germ cell development [52] and skeletal muscle aging through DNA hypomethylation [53, Shang et al.]. Three down-regulated miRNAs (miR-375-3p, miR-30e-3p, and miR-26b-5p) were also identified by another study on ApoE<sup>-/-</sup> mice fed with a Western-type diet for 8 months [35]. The whole miR-375-3p was found up-regulated

in a previous study; it was down-regulated in our study. Even though there is no specific report of miR-375-3p on atherosclerosis, it was reported to be up-regulated in angiotensin II-induced primary cardiomyocyte hypertrophy rats [54]. Fu and his colleagues demonstrated that exosomal mmu-miR-375-3p was dramatically increased in the serum of an STZ treated mouse prior to the disturbance of blood glucose and insulin [55]. Knudsen considered miR-375 as a potential regulator of the enteroendocrine lineage [56]. Another researcher revealed that miR-375-3p negatively modulated osteogenesis, and the relevant products of miR-375-3p might be developed into potential molecular drugs [57].

MiR-382-5p was reported to be involved in the regulation of cholesterol homeostasis and inflammatory reactions [58] and in many other diseases like glioma cell proliferation, migration and invasion [59], breast cancer [60], glioma angiogenesis [61], acute promyelocytic leukemia (Liu et al. 2019a), and primary myelofibrosis [62]. Among

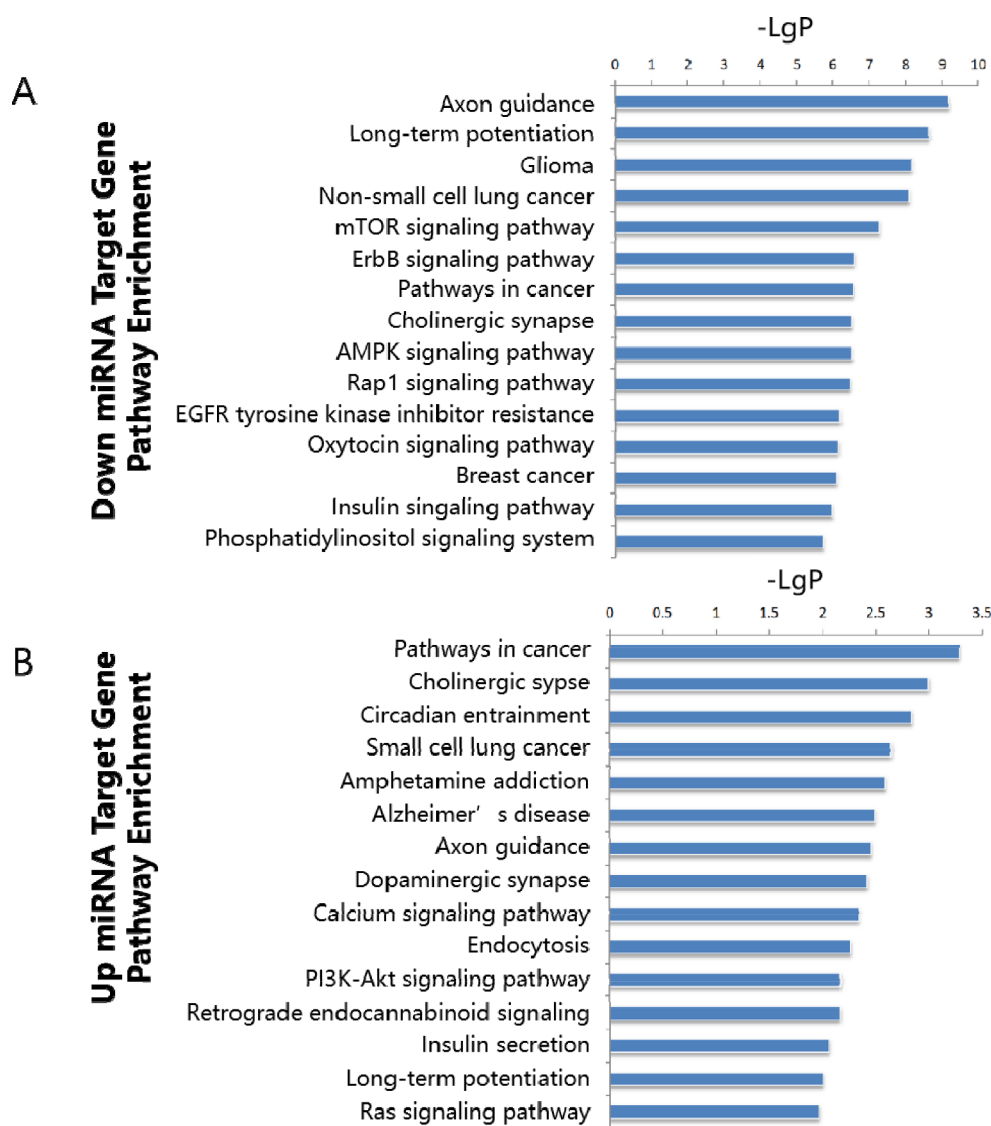


**Figure 5.** Summary of significantly enriched pathways. A: Target genes of downregulated miRNAs. B: Target genes of upregulated miRNA.

another 5 downregulated miRs (miR-329-3p, miR-379-5p, miR-7a-5p, miR-674-3p, and miR-138-5p) with fold change less than 3 in this study, miR-329-3p was identified as upregulated in the progression of diabetic atherosclerotic rat [63], and miR-379-5p has been reported to play an important regulatory role in the proliferation and migration of many tumor cells [64–67]. There are no reports on the pathogenesis of atherosclerosis involving miR-7a-5p, miR-674-3p, miR-6239, miR-7671-3p, miR-674-3p, miR-138-5p, and miR-7001-5p. MiR-7001-5p is the only upregulated microRNA identified in this study, and its role in atherosclerosis is not clear.

Short non-coding miRNAs are gene silencers that exert biological effects through gene expression regulation of target genes participating in multiple signaling pathways notoriously involved in atherosclerosis, like phosphatidylinositol 3-kinase/serine/threonine kinase 1/mammalian target of rapamycin (PI3K/Akt/mTOR), mitogen-activated protein kinase (MAPK), Ras homolog gene family, member A/ (RhoA/ROCK), transforming growth factor-beta (TGF-beta), epidermal growth factor receptor (EGFR), Nuclear Factor-KappaB (NF-kappaB), Janus kinase 1/signal transducer and activator of transcription 1 (JAK1/STAT1), Notch and Wnt signaling pathways, etc



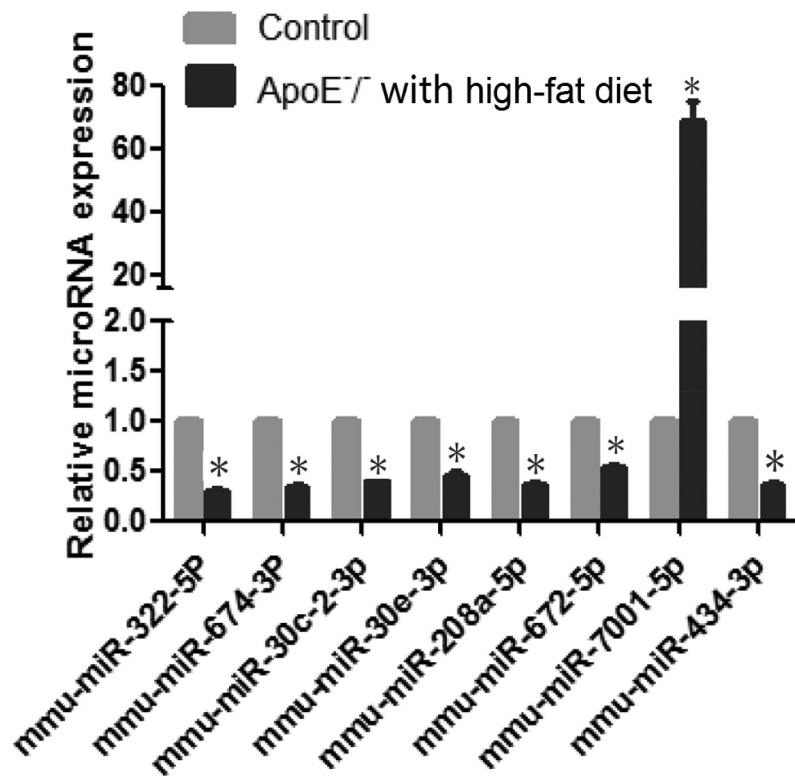


**Figure 6.** Real-Time qPCR validation of selected miRNAs. \* $p < 0.01$ .

**Table 3.** Differentially expressed microRNAs with a high significance ( $p < 0.05$ , fold change  $\geq 2.0$ ).

Probe set	Transcript.ID.Array.Design.	fold change	<i>P</i> .Value	Regulation
MIMAT0000739_st	mmu-miR-434-3p	-13.93994	0.018375	down
MIMAT0000747_st	mmu-miR-382-5p	-5.961757	0.002912	down
MIMAT0001422_st	mmu-miR-329-3p	-3.988368	0.002183	down
MIMAT0000743_st	mmu-miR-379-5p	-3.381547	0.006986	down
MIMAT0000677_st	mmu-miR-7a-5p	-3.308576	0.012732	down
MIMAT0003741_st	mmu-miR-674-3p	-3.262847	0.001639	down
MIMAT0000150_st	mmu-miR-138-5p	-3.262847	0.001639	down
MIMAT0000534_st	mmu-miR-26b-5p	-3.105263	0.01418	down
MIMAT0003735_st	mmu-miR-672-5p	-2.968656	0.036304	down
MIMAT0000609_st	mmu-miR-351-5p	-2.816603	0.003982	down
MIMAT0004644_st	mmu-miR-337-5p	-2.770042	0.000285	down
MIMAT0025110_st	mmu-miR-6366	-2.676591	0.040688	down
MIMAT0000545_st	mmu-miR-98-5p	-2.664066	0.001186	down
MIMAT0017014_st	mmu-miR-208a-5p	-2.608746	0.015035	down
MIMAT0004747_st	mmu-miR-411-5p	-2.446921	0.006458	down
MIMAT0005438_st	mmu-miR-30 c-2-3p	-2.438473	0.00091	down
MIMAT0000548_st	mmu-miR-322-5p	-2.392655	0.002247	down
MIMAT0029849_st	mmu-miR-7671-3p	-2.367063	0.02349	down
MIMAT0000249_st	mmu-miR-30e-3p	-2.298771	0.001399	down
MIMAT0017059_st	mmu-miR-211-3p	-2.111502	0.006546	down
MIMAT0024860_st	mmu-miR-6239	-2.056051	0.023371	down
MIMAT0025580_st	mmu-let-7k	-2.032289	0.00467	down
MIMAT0000208_st	mmu-miR-10b-5p	-2.027658	0.009782	down
MIMAT0027904_st	mmu-miR-7001-5p	2.9272093	0.0131507	up

[26,38,68–72]. In the present study, both the GO and KEGG pathway enrichment analysis identified high enrichment of target genes involved in the PI3K/Akt/mTOR, Adenosine Monophosphate

Activated Protein Kinase (AMPK)/MAPK, Wnt, Notch, insulin, and the NF-kappaB signaling pathways, and the PI3K/Akt/mTOR signaling pathway was identified in both upregulated and

downregulated miRs target genes. Our data confirm the correct identification of more dysregulated miRs in atherosclerosis.

This study bears the limitation of one-time point sampling. Therefore, additional systematic experiments are needed to verify the mechanism of miRNAs on atherosclerosis.

## Conclusions

This study has identified 25 differentially expressed miRs, including a set of novel miRs involved in atherosclerogenesis using GeneChip microarray profiling of miRs in high-fat-fed ApoE<sup>-/-</sup> mice fed with a high-fat diet, and bioinformatic analysis reveals that the PI3K/Akt/mTOR signaling pathway is highly enriched in the predicted target genes [73]. The novel identified dysregulated miRs suggest a broad spectrum of miRs dysregulation in the progression of atherosclerosis and provide additional research and therapeutic targets [74].

## Highlights

- A total of 25 significant differentially expressed microRNAs were identified.
- In atherosclerosis, miR-701-5p expression is up-regulated.
- The PI3K/Akt/mTOR signaling pathway is highly involved in atherosclerosis.

## Acknowledgements

The authors acknowledge the teachers and students of experimental pharmacology and toxicology laboratory, College of Pharmacy of Jilin University for their great support and help.

## Contributions

Xiaoqian Lou and Liqun Ren designed the research; Dawei Wang conducted the experiments; Zehui Gu interpreted the results and referred to the references; Xiaoqian Lou wrote the manuscript and Liqun Ren edited the manuscript.

## Disclosure statement

No potential conflict of interest was reported by the author(s).

## Funding

This work was supported by the National Natural Science Foundation of China (81773934).

## References

- [1] Flora GD, Nayak MK. A brief review of cardiovascular diseases, associated risk factors and current treatment regimes. *Curr Pharm Des.* 2019;25(38):4063–4084.
- [2] Mozaffarian D, Mozaffarian D, Benjamin EJ, et al. Heart disease and stroke statistics-2016 update: a report from the American Heart Association. *Circulation.* 2016;133(4):e38–360.
- [3] Gimbrone MA Jr., Garcia-Cardena G. Endothelial cell dysfunction and the pathobiology of atherosclerosis. *Circ Res.* 2016;118(4):620–636.
- [4] Paone S, Baxter AA, Hulett MD, et al. Endothelial cell apoptosis and the role of endothelial cell-derived extracellular vesicles in the progression of atherosclerosis. *Cell Mol Life Sci.* 2019;76(6):1093–1106.
- [5] Bories GFP, Leitinger N. Macrophage metabolism in atherosclerosis. *FEBS Lett.* 2017;591(19):3042–3060.
- [6] Groh L, Keating ST, Joosten LAB, et al. Monocyte and macrophage immunometabolism in atherosclerosis. *Semin Immunopathol.* 2018;40(2):203–214.
- [7] Chistiakov DA, Orekhov AN, Bobryshev YV. Vascular smooth muscle cell in atherosclerosis. *Acta Physiol (Oxf).* 2015;214(1):33–50.
- [8] Wang Y, et al. Smooth muscle cells contribute the majority of foam cells in ApoE (Apolipoprotein E)-deficient mouse atherosclerosis. *Thromb Vasc Biol Atvbah* 2019b;a119312434.
- [9] Hurtubise J, McLellan K, Durr K, et al. the different facets of dyslipidemia and hypertension in atherosclerosis current atherosclerosis reports 18:82 hussain MM, Goldberg IJ (2018) Human MicroRNA-33b Promotes Atherosclerosis in Apoe(-/-) Mice. *Arterioscler Thromb Vasc Biol.* 2016;38:2272–2275.
- [10] Koelwyn GJ, Corr EM, Erbay E. Regulation of macrophage immunometabolism in atherosclerosis. *Nat Immunol.* 2018;19(6):526–537.
- [11] Low Wang CC, Hess CN, Hiatt WR, et al. Clinical update: cardiovascular disease in diabetes mellitus: atherosclerotic cardiovascular disease and heart failure in type 2 diabetes mellitus - mechanisms, management, and clinical considerations. *Circulation.* 2016;133(24):2459–2502.
- [12] Marchio P, Guerra-Ojeda S, Vila JM. Targeting early atherosclerosis: a focus on oxidative stress and inflammation. *Oxid Med Cell Longev.* 2019;2019:8563845.
- [13] Shimada K. Immune system and atherosclerotic disease: heterogeneity of leukocyte subsets participating in the pathogenesis of atherosclerosis. *Circ J.* 2009;73(6):994–1001.

- [14] Bartel DP. MicroRNAs: genomics, biogenesis, mechanism, and function. *Cell*. 2004;116(2):281–297.
- [15] Eastwood J, Caslake MJ, Sodi R. The association of circulating microRNA-30c with atherogenic lipoprotein subfractions and composition *Clinica chimica acta. Int J Clin Chem*. 2016;462:135–139.
- [16] Feinberg MW, Moore KJ. MicroRNA Regulation of Atherosclerosis. *Circ Res*. 2016;118(4):703–720.
- [17] Tana C, Giamberardino MA, Cipollone F. microRNA profiling in atherosclerosis, diabetes, and migraine. *Ann Med*. 2017;49(2):93–105.
- [18] Wang A, Kwee LC, Grass E, et al. Whole blood sequencing reveals circulating microRNA associations with high-risk traits in non-ST-segment elevation acute coronary syndrome. *Atherosclerosis*. 2017a;261:19–25.
- [19] Li Y, Yang N, Dong B, et al. MicroRNA-122 promotes endothelial cell apoptosis by targeting XIAP: therapeutic implication for atherosclerosis. *Life Sci*. 2019;232:116590.
- [20] Menghini R, Casagrande V, Marino A, et al. MiR-216a: a link between endothelial dysfunction and autophagy. *Cell Death Dis*. 2014;5(1):e1029.
- [21] Zhao J, Ou SL, Wang WY, et al. MicroRNA-1907 enhances atherosclerosis-associated endothelial cell apoptosis by suppressing Bcl-2. *Am J Transl Res*. 2017;9(7):3433–3442.
- [22] Zhu L, Li Q, Qi D, et al. Atherosclerosis-associated endothelial cell apoptosis by miRNA let7-b-mediated downregulation of HAS-2. *J Cell Biochem*. 2019 Nov;2019:17.
- [23] Di Gregoli K, Jenkins N, Salter R, et al. MicroRNA-24 regulates macrophage behavior and retards atherosclerosis. *Arterioscler Thromb Vasc Biol*. 2014;34(9):1990–2000.
- [24] Karunakaran D, Rayner KJ. Macrophage miRNAs in atherosclerosis. *Biochim Biophys Acta*. 2016;1861(1):2087–2093.
- [25] Ouimet M, Ediriweera H, Afonso MS, et al. microRNA-33 Regulates Macrophage Autophagy in Atherosclerosis. *Arterioscler Thromb Vasc Biol*. 2017;37(6):1058–1067.
- [26] Yang S, et al. MicroRNA-216a promotes M1 macrophages polarization and atherosclerosis progression by activating telomerase via the Smad3/NF-kappaB pathway. *Biochim Biophys Acta Mol Basis Dis*. 2019;1865(7):1772–1781.
- [27] Alshanwani AR, Riches-Suman K, O'Regan DJ, et al. MicroRNA-21 drives the switch to a synthetic phenotype in human saphenous vein smooth muscle cells. *IUBMB Life*. 2018;70(7):649–657.
- [28] Liu H, Xiong W, Liu F, et al. Dong S(2019b) MicroRNA-133b regulates the growth and migration of vascular smooth muscle cells by targeting matrix metalloproteinase 9. *Pathol Res Pract*. 2019;215(5):1083–1088.
- [29] Sun Y, Gao Y, Song T, et al. MicroRNA-15b participates in the development of peripheral arterial disease by modulating the growth of vascular smooth muscle cells. *Exp Ther Med*. 2019;18(1):77–84.
- [30] Xing T, Du L, Zhuang X, et al. Upregulation of microRNA-206 induces apoptosis of vascular smooth muscle cells and decreases risk of atherosclerosis through modulating FOXP1. *Exp Ther Med*. 2017;14(5):4097–4103.
- [31] Zahedi F, et al. Dicer generates a regulatory microRNA network in smooth muscle cells that limits neointima formation during vascular repair. *Cell Mol Life Sci*. 2017;74(2):359–372.
- [32] Ren K, Zhu X, Zheng Z, et al. MicroRNA-24 aggravates atherosclerosis by inhibiting selective lipid uptake from HDL cholesterol via the post-transcriptional repression of scavenger receptor class B type I. *Atherosclerosis*. 2018;270:57–67.
- [33] Sahebkar A, Watts GF. Developing role of microRNA-33 in lipid metabolism and atherosclerosis. *Curr Opin Lipidol*. 2016;27(2):197–199.
- [34] Tan L, Liu L, Jiang Z, et al. Inhibition of microRNA-17-5p reduces the inflammation and lipid accumulation, and up-regulates ATP-binding cassette transporterA1 in atherosclerosis. *J Pharmacol Sci*. 2019;139(4):280–288.
- [35] Han H, Wang Y-H, Qu G-J, et al. Differentiated miRNA expression and validation of signaling pathways in apoE gene knockout mice by cross-verification microarray platform. *Exp Mol Med*. 2013;45(3):e13.
- [36] Zhen S, Yao C, Li Z-L, et al. Differentially expressed microRNAs at different stages of atherosclerosis in ApoE-deficient mice. *Chin Med J (Engl)*. 2013;126(3):515–520.
- [37] Virtue A, Johnson C, Lopez-Pastrana J, et al. MicroRNA-155 deficiency leads to decreased atherosclerosis, increased white adipose tissue obesity, and non-alcoholic fatty liver disease: a NOVEL MOUSE MODEL OF OBESITY PARADOX. *J Biol Chem*. 2017;292(4):1267–1287.
- [38] Jing R, Zhong QQ, Long TY, et al. Downregulated miRNA-26a-5p induces the apoptosis of endothelial cells in coronary heart disease by inhibiting PI3K/AKT pathway. *Eur Rev Med Pharmacol Sci*. 2019;23(11):4940–4947.
- [39] Zhang Y, Ma X, Li X, et al. Effects of icariin on atherosclerosis and predicted function regulatory network in apoE deficient mice. *Biomed Res Int*. 2018b;2018:9424186.
- [40] Lin Y, Bai L, Chen Y, et al. Liu E(2015) Practical assessment of the quantification of atherosclerotic lesions in apoE<sup>-/-</sup>-mice. *Mol Med Rep*. 2015;12(4):5298–5306.
- [41] Papadaki C, Monastirioti A, Rounis K, et al. Circulating MicroRNAs regulating DNA damage response and responsiveness to cisplatin in the prognosis of patients with non-small cell lung cancer treated with first-line platinum chemotherapy. *Cancers (Basel)*. 2020;12(5):1282.
- [42] Agarwal V, Bell GW, Nam JW, et al. (2015) Predicting effective microRNA target sites in mammalian mRNAs *Elife* 4

- [43] Betel D, Wilson M, Gabow A, et al. The microRNA.org resource: targets and expression. *Nucleic Acids Res.* **2008**;36(Database):D149–153.
- [44] Lydersen S, Laake P. Power comparison of two-sided exact tests for association in  $2 \times 2$  contingency tables using standard, midp and randomized test versions. *Stat Med.* **2003**;22(24):172643–172671.
- [45] McHugh ML. The chi-square test of Independence. *Biochem Med (Zagreb).* **2013**;23(2):143–149.
- [46] Mishra P, Singh U, Pandey CM, et al. Application of student's t-test, analysis of variance, and covariance. *Ann Card Anaesth.* **2019**;22(4):407–411.
- [47] Getz GS, Reardon CA. Diet and murine atherosclerosis. *Arterioscler Thromb Vasc Biol.* **2006**;26(2):242–249.
- [48] Getz GS, Reardon CA. Diet, microbes, and murine atherosclerosis. *Arterioscler Thromb Vasc Biol.* **2018**;38(10):2269–2271.
- [49] Chipont A, Esposito B, Challier I, et al. MicroRNA-21 deficiency alters the survival of Ly-6C lo monocytes in ApoE<sup>-/-</sup> mice and reduces early-stage Atherosclerosis —Brief Report. *Arterioscler Thromb Vasc Biol.* **2019**;39(2):170–177.
- [50] Ye Y, Zhao X, Lu Y, et al. Varinostat Alters Gene Expression Profiles in Aortic Tissues from ApoE<sup>-/-</sup> Mice. *Ther Clin Dev.* **2018**;29(4):214–225
- [51] Yerlikaya FH, Ö M. Aberrant expression of miRNA profiles in high-fat and high-sucrose fed rats. *Clin Nutr Exp.* **2019**;27:1–8.
- [52] Chen H, Guo X, Xiao X, et al. Identification and functional characterization of microRNAs in rat Leydig cells during development from the progenitor to the adult stage. *Mol Cell Endocrinol.* **2019**;493:110453.
- [53] Pardo PS, Hajira A, Boriek AM, et al. MicroRNA-434-3p regulates age-related apoptosis through eIF5A1 in the skeletal muscle. *Aging (Albany NY).* **2017**;9(3):1012–1029.
- [54] Feng H, Wu J, Chen P, et al. MicroRNA-375-3p inhibitor suppresses angiotensin II-induced cardiomyocyte hypertrophy by promoting lactate dehydrogenase B expression. *J Cell Physiol.* **2019**;234(8):14198–14209.
- [55] Fu Q, Jiang H, Wang Z, et al. Injury factors alter miRNAs profiles of exosomes derived from islets and circulatio. *Aging (Albany NY).* **2018**;10(12):3986–3999.
- [56] Knudsen LA, Petersen N, Schwartz TW, et al. The MicroRNA repertoire in enteroendocrine cells: identification of miR-375 as a potential regulator of the enteroendocrine lineage. *Endocrinology.* **2015**;156(11):3971–3983.
- [57] Sun T, Li CT, Xiong L, et al. miR-375-3p negatively regulates osteogenesis by targeting and decreasing the expression levels of LRP5 and beta-catenin. *PLoS One.* **2017**;12:e0171281.
- [58] Hu YW, Zhao J-Y, Li S-F, et al. RP5-833A20.1/miR-382-5p/NFIA-dependent signal transduction pathway contributes to the regulation of cholesterol homeostasis and inflammatory reaction. *Arterioscler Thromb Vasc Biol.* **2015**;35(1):87–101.
- [59] Wang J, Chen C, Yan X, et al. The role of miR-382-5p in glioma cell proliferation, migration and invasion. *Onco Targets Ther.* **2019a**;261:4993–5002.
- [60] Zheng S, Li M, Miao K, et al. SNHG1 contributes to proliferation and invasion by regulating miR-382 in breast cancer. *Cancer Manag Res.* **2019**;11:5589–5598.
- [61] He Q, Zhao L, Liu X, et al. MOV10 binding circ-DICER1 regulates the angiogenesis of glioma via miR-103a-3p/miR-382-5p mediated ZIC4 expression change. *J Exp Clin Cancer Res.* **2019b**;38(1):9.
- [62] Rossi C, Zini R, Rontautoli S. Role of TGF- $\beta$ 1/miR-382-5p/SOD2 axis in the induction of oxidative stress in CD 34+ cells from primary myelofibrosis. *Mol Oncol.* **2018**;12(12):2102–2123.
- [63] Li Y, Xiao L, Li J, et al. MicroRNA profiling of diabetic atherosclerosis in a rat model. *Eur J Med Res.* **2018**;23(1):55.
- [64] Chen JS, Huang JQ, Dong SH, et al. [Effects of microRNA-379-5p on proliferation, migration and invasion of hepatocellular carcinoma cell line]. *Zhonghua Yi Xue Za Zhi.* **2016**;96(18):1450–1453.
- [65] He Q, Fang Y, Lu F. Analysis of differential expression profile of miRNA in peripheral blood of patients with lung cancer. *J Clin Lab Anal.* **2019a**;33(9):e23003.
- [66] Lv X, Wang M, Qiang J, et al. Circular RNA circ-PITX1 promotes the progression of glioblastoma by acting as a competing endogenous RNA to regulate miR-379-5p/MAP3K2 axis. *Eur J Pharmacol.* **2019**;863:172643.
- [67] Xu X, Wang Y, Mojumdar K, et al. A-to-I-edited miRNA-379-5p inhibits cancer cell proliferation through CD97-induced apoptosis. *J Clin Invest.* **2019**;129(12):5343–5356.
- [68] Gao ZF, Ji XL, Gu J, et al. microRNA-107 protects against inflammation and endoplasmic reticulum stress of vascular endothelial cells via KRT1-dependent Notch signaling pathway in a mouse model of coronary atherosclerosis. *J Cell Physiol.* **2019**;234(7):12029–12041.
- [69] Hao XZ, Fan HM. Identification of miRNAs as atherosclerosis biomarkers and functional role of miR-126 in atherosclerosis progression through MAPK signalling pathway. *Eur Rev Med Pharmacol Sci.* **2017**;21(11):2725–2733.
- [70] Tang F, Yang TL. MicroRNA-126 alleviates endothelial cells injury in atherosclerosis by restoring autophagic flux via inhibiting of PI3K/Akt/mTOR pathway. *Biochem Biophys Res Commun.* **2018**;495(1):1482–1489.
- [71] Wang Y, Han Z, Fan Y, et al. MicroRNA-9 Inhibits NLRP3 inflammasome activation in human atherosclerosis inflammation cell models through the JAK1/STAT signaling pathway. *Cell Physiol Biochem.* **2017b**;41(4):1555–1571.

- [72] Zhang Y, Jia L, Ji W, et al. MicroRNA-141 inhibits the proliferation of penile cavernous smooth muscle cells associated with down-regulation of the rhoa/rho kinase signaling pathway. *Cell Physiol Biochem*. 2018a;48(1):348–360.
- [73] Liu D, Zhong L, Yuan Z, et al. Liu B(2019a) miR-382-5p modulates the ATRA-induced differentiation of acute promyelocytic leukemia by targeting tumor suppressor PTEN. *Cell Signal*. 2019;54:1–9.
- [74] Shang FF, Xia QJ, Liu W, et al. miR-434-3p and DNA hypomethylation co-regulate eIF5A1 to increase AChRs and to improve plasticity in SCT rat skeletal muscle. *Sci Rep*. 2016;6(1):22884.